

A novel naturally occurring tripyrrole with potential nuclease and anti-tumour properties

Mahesh Subramanian,^a Ramesh Chander^b and Subrata Chattopadhyay^{a,*}

^aBio-Organic Division, Bhabha Atomic Research Centre, Mumbai 400 085, India

^bFood Technology Division, Bhabha Atomic Research Centre, Mumbai 400 085, India

Received 29 March 2005; accepted 15 November 2005

Available online 10 January 2006

Abstract—The DNA targeting and membrane damaging activities of a novel tripyrrole **1** obtained as a red pigment from the *Micrococcus* sp. were investigated. It was found that compound **1** binds with DNA efficiently and facilitates copper-mediated DNA cleavage as well as peroxidation of membrane lipids by a process that does not require any external reducing agent. Compound **1** also showed impressive cytotoxicity to both mouse and human tumour cell lines. The membrane damaging ability of compound **1** might be vital in its nuclease and cytotoxicity properties. Interestingly, compared to the various DNA cleaving agents, compound **1** showed a preferential binding with the G–C rich domain.

© 2005 Elsevier Ltd. All rights reserved.

1. Introduction

There is a burgeoning interest in small organic molecules that are especially capable of binding to specific DNA sequences and cleaving DNA as these can be used in the design and development of new drugs, synthetic restriction enzymes, DNA footprinting agents, etc.^{1–3} Towards this end, several DNA targeting agents like DAPI, furamidine and DNA cleavers like bleomycin, polypyrroles, etc., have been developed. However, amongst these, the prodigiosins assume the most significant position due to their potential anti-cancer properties.⁴

Recently, we have isolated a novel prodigiosin analogue (**1**) (Fig. 1) as a red pigment from the *Micrococcus* sp. obtained from sterilized dehydrated shrimp.⁵ In addition to their susceptibility to oxidation,⁶ this type of tripyrrole contains suitable structural features for DNA binding, and hence shows metal-mediated nuclease activity.^{7,8} However, compared to the prodigiosins, compound **1** is not completely planar and as an N-alkylated analogue, it is anticipated to be more hydrophobic. Structural comparison between prodigiosins and the new tripyrrole **1** is shown in Figure 1. Thus, it was

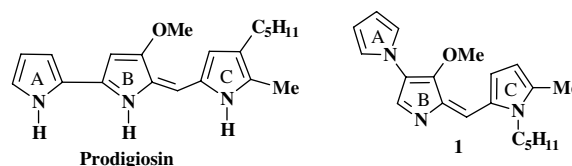


Figure 1. Structures of prodigiosin and the tripyrrole **1**.

anticipated to show different DNA binding and oxidative properties. Consequently, in view of our own interest in this area,⁹ we studied its nuclease and membrane damaging potential and the interesting results are presented in this paper. The primary aim of this investigation was to evaluate its in vitro biological activity for a further evaluation of its cytotoxic property.

2. Results and discussion

2.1. Cu(II) and DNA binding capacities of compound **1**

The absorption spectroscopic studies revealed that compound **1** forms chelate with Cu(II), with an absorption maximum at 540 nm. Compound **1** was also found to bind efficiently with DNA and DNA segments, as addition of CT DNA, poly[A–T]₂ and poly[G–C]₂ in increasing amounts to a fixed concentration of **1** (20 μM) led to gradual reduction in the intensities of the absorption bands (502 and 540 nm) of free **1** and caused a minor

Keywords: Copper; DNA; Prodigiosin analogue; Nuclease; Redox.

* Corresponding author. Fax: +91 22 25505151; e-mail: schatt@apsara.barc.ernet.in

Table 1. Comparative binding constants (K) of **1** with nucleic acids

Compound	Nucleic Acid	Binding constant, K (M^{-1})
1	CT DNA	3.3×10^5
1	Poly[A–T] ₂	1.5×10^5
1	Poly[G–C] ₂	1.1×10^6
EB	CT DNA	2.5×10^5

The UV–vis titrations were carried out with CT DNA, poly[A–T]₂ and poly[G–C]₂ in 10 mM Hepes buffer, pH 7.2, by adding different base pair aliquots as described in Section 4. EB was used as a control.

red-shift (1.5–3 nm). This kind of red-shift of the absorption maxima due to the stacking of metabolites of polycyclic aromatic hydrocarbons with DNA bases has earlier been reported.^{10a,b} The equilibrium DNA binding constant (K) values of 10^5 – 10^7 M^{-1} for **1** in respective cases (Table 1) were similar to those of typical intercalators¹¹ and revealed that the G–C domain binding of **1** was ~ 7.5 -fold stronger than that with the A–T domain. The K values for its binding with CT DNA and poly[A–T]₂ were similar in magnitude. The K value for the binding of the known DNA intercalator, ethidium bromide (EB) with CT DNA was also of the same order as that of **1** (Table 1). Regression analysis in all the cases showed linear fits indicative of a single mode binding of **1** with DNA.

Further indication of the intercalative DNA binding by **1** was also obtained by the EB fluorescence quenching assay. Due to its strong intercalation between the adjacent DNA base pairs, EB emits intense fluorescence in the presence of DNA. The enhanced fluorescence can be quenched by the addition of a second intercalating molecule and the extent of fluorescence quenching can be used to quantify the binding of the second molecule and DNA.^{12a,b} The emission spectra of EB bound to DNA in the absence and presence of **1** are shown in Figure 2. As it is evident, in the presence of **1** (0.1 mM) the EB fluorescence was quenched considerably ($\sim 40\%$), indicating its intercalative binding with DNA.

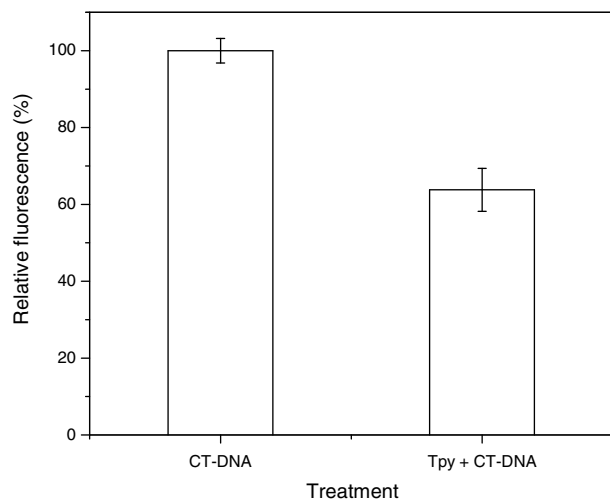


Figure 2. Quenching of EB fluorescence by tripyrrole. The fluorescence of EB bound to CT DNA in the presence and absence of tripyrrole was measured at emission 600 nm after excitation at 530 nm. The reduction in fluorescent intensity is expressed as the percentage of that of control (CT DNA + EB; values are means \pm SE, $n = 4$).

The intercalating DNA binding by **1** was finally confirmed by measuring the change in the viscosity of DNA solution in its presence.^{13a,b} A classical intercalative binding mode causes a significant increase in the viscosity of DNA solution due to an increase in the separation of base pairs at intercalation sites resulting in an increase in the overall DNA length. In contrast, complexes that bind exclusively in the DNA grooves by partial and/or non-classical intercalation, typically cause less or no change in the viscosity of the DNA solution.^{13c}

For this study, the viscosity of a fixed concentration of CT DNA (0.2 mM) was measured in the presence of increasing concentrations of **1**. The concentration of **1** was increased for a R value of 0–1, where $R = [\text{compound } 1]/[\text{DNA}]$. As shown in Figure 3, the increase in the R value led to higher viscosity of the DNA solution, confirming an intercalative mode of DNA binding by **1**. The results are in conformity with those reported with its structural congener, prodigiosins.^{7,14a,b}

Compound **1** possesses unfused aromatic ring systems bearing cationic charge at physiological pH. The cationic property of **1** appears to be critical for its efficient binding with DNA. All these argued in favour of an intercalative, groove binding of **1** with DNA via ion-pair interaction. Weakening of the binding with increased NaCl concentration (100–500 mM) further confirmed it.

The G–C specificity of **1** is very interesting given that the polypyrroles including the prodigiosins are known to bind with A–T specificity.^{7,8} While the structural origin of the binding site preference of **1** is unclear, contributions from hydrogen-bonding (H-B), electrostatic and other weak interactions are anticipated. The poor solubility of **1** in water and lack of its fluorescence precluded

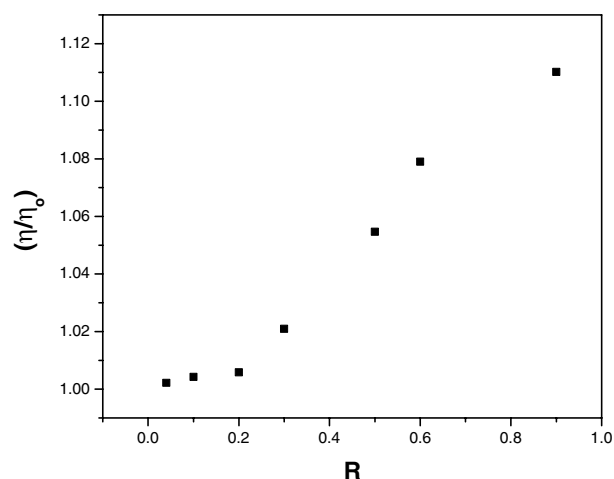


Figure 3. Viscometry measurement of CT DNA solution in the presence of different concentrations of tripyrrole. Different R ([tripyrrrole]/[DNA base pairs]) values were obtained by addition of tripyrrole to 0.2 mM CT DNA solution in 10 mM Hepes buffer with 100 mM NaCl. The flow times of the samples were measured at least three times. The data obtained are presented as (η/η_0) versus R , where η is the reduced specific viscosity of CT DNA in the presence of tripyrrole and η_0 is the reduced specific viscosity of CT DNA alone.

a detailed study on its binding with DNA. The A–T specific binding of the prodigiosins is primarily explained by the hydrogen-bonding interactions of the pyrrole NH group to the N and O atoms of the AT base pair.⁷ In addition, favourable electrostatic interactions arising out of their cationic nature and negative potential of the A–T sequence play a minor role. Such an interaction would be absent with the tripyrrole **1** as it lacks any pyrrole NH group. Instead, like other unfused aromatic cations such as DAPI^{15a} and furamidine,^{15b} it can bind at the G–C site by intercalation where it would have favourable π -stacking interactions with the DNA base pairs. In contrast to the prodigiosins, only the 'B' and 'C' rings of compound **1** are conjugated and planar. The alkyl group and the 'A' ring appear as appendages to the planar 'B'–'C' rings aromatic system that is responsible for the intercalation. This would allow the planar 'B'–'C' rings to slide into the G–C domain, with the appendages protruding out, thus alleviating the steric strain.

2.2. DNA cleavage capacity of **1**

The ability of compound **1** to mediate DNA cleavage was assessed using agarose gel electrophoresis and

supercoiled plasmid pBR 322 DNA (form I). As shown in Figure 4a, both Cu(II) and **1** are required for the DNA strand scission (lane 3), while they could not cleave DNA individually (lanes 1 and 2). Compound **1** did not show nuclease property in the presence of other metal ions like Fe(III), Ni(II), and Zn(II) or in the absence of oxygen (data not shown). The cleavage was complete with equimolar concentrations of Cu(II), while lowering the Cu(II) concentration progressively reduced the extent of DNA strand scission. The single strand cleavage was complete within 30 min (lanes 3–7), while significant double-strand DNA (dsDNA) cleavage^{16a,b} appeared after ~60 min as revealed from all the three forms of DNA in lanes 5–7. Increasing the incubation beyond 2 h led to the appearance of multiple DNA bands. After ~3 h instead of any band, complete smearing of DNA was seen (data not shown), revealing multiple sites of damage. In experiments carried out at two incubation periods (15 and 30 min), the alkali labile sites were clearly visible (Fig. 4b), suggesting that compound **1** could also damage the DNA bases effectively.

The effects of various scavengers of reactive oxygen species (ROS) and metal ion chelators on the nuclease activity of **1** are shown in Figure 4c. The cleavage was

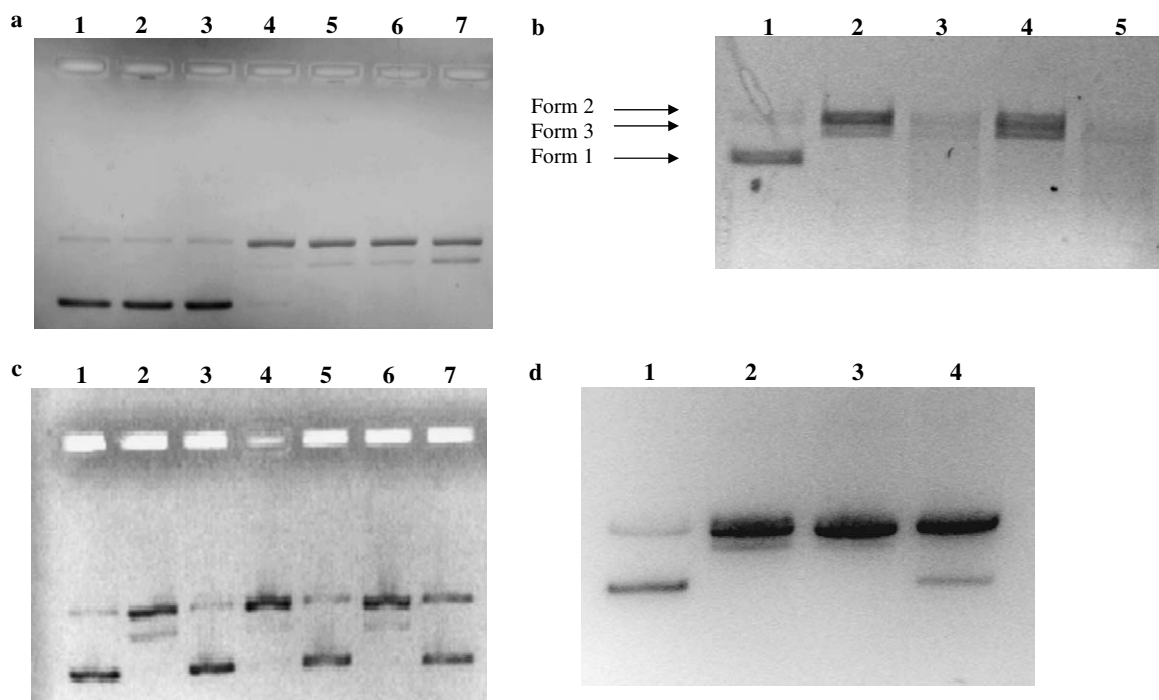


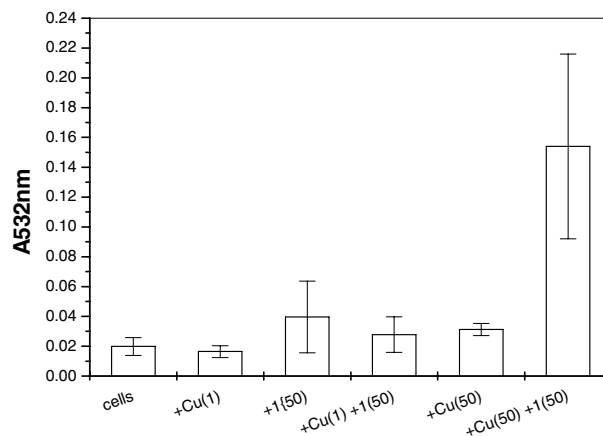
Figure 4. (a) Gel electrophoresis pattern of supercoiled plasmid DNA (form I) cleavage by **1** (50 μM) + Cu²⁺ (50 μM) after different times of incubation at 37 °C. Reaction mixture (20 μL, total volume) contained 200 ng of form I DNA in 10 mM Hepes buffer, pH 7.4, and Cu(OAc)₂ (50 μM). Other conditions are as described in Section 4. Lane 1, DNA + Cu²⁺; lane 2, DNA + **1**; lanes 3–7, DNA + **1** + Cu²⁺ (0, 30, 60, 90 and 120 min, respectively). (b) Detection of alkali labile sites after the plasmid DNA (form I) cleavage by **1** (100 μM) + Cu(OAc)₂ (100 μM). Other conditions are as described for Figure 2a and in Section 4. Lane 1, DNA alone; lanes 2, 3, DNA + **1** + Cu²⁺, 15 min incubation; lanes 4, 5, DNA + **1** + Cu²⁺, 30 min incubation; lanes 3, 5, NaOH (0.5 M) was added prior to gel electrophoresis. (c) Effect of different inhibitors on supercoiled plasmid DNA (form I) cleavage by **1** + Cu(OAc)₂ after 60 min incubation at 37 °C. The experimental conditions are as described for Figure 2a and in Section 4. Lane 1, DNA alone; lane 2, DNA + **1** + Cu²⁺; lane 3, DNA + **1** + Cu²⁺ + EDTA (100 mM); lane 4, DNA + **1** + Cu²⁺ + DMSO (1 M); lane 5, DNA + **1** + Cu²⁺ + catalase (1000 U/mL); lane 6, DNA + **1** + Cu²⁺ + SOD (1000 U/mL); lane 7, DNA + **1** + Cu²⁺ + NaN₃ (100 mM). (d) Effect of different concentrations of bathocuproine on supercoiled plasmid DNA (form I) cleavage by **1** + Cu(OAc)₂ after 60 min incubation at 37 °C. The conditions are as described for Figure 2a and in Section 4. Lane 1, DNA alone; lane 2, DNA + **1** + Cu²⁺; lanes 3, 4, DNA + **1** + Cu²⁺ + bathocuproine (50 and 100 μM) respectively.

not affected by the ROS scavengers like DMSO and SOD (for $\cdot\text{OH}$ and $\text{O}_2^{\cdot-}$, respectively), excluding participation of these diffusible ROS in the process. Although sodium azide, a $^1\text{O}_2$ quencher, reduced the DNA damage (lane 7), the possible participation of the ROS could be excluded from the fact that the damage did not increase (data not shown) in D_2O , which is known to increase the lifetime of $^1\text{O}_2$. The anomalous results could be explained as follows. The inhibitory effect of NaN_3 might not be due to the $^1\text{O}_2$ quencher, azide ions. Instead, the increased concentration of Na^+ ions might contribute to the lesser nuclease activity of **1** by reducing its DNA binding capacity, as was observed with NaCl . However, EDTA (metal chelator) and catalase could prevent the cleavage (lanes 3 and 5) significantly. Bathocuproine, a Cu(I) -specific chelator, prevented the DNA scission in a concentration dependent manner (Fig. 4d).

Thus, the cleavage was oxidative and revealed the intermediacy of a Cu(I) -peroxo compound as has been reported earlier by us with hydroxystilbenes⁹ and others for polypyrroles.^{7,8} Mechanistically, Cu(II) -catalyzed oxidation of compound **1** furnished a π -radical polypyrrole cationic intermediate and Cu(I) . The polypyrrole intermediate would then dimerize very fast. However, the Cu(I) produced would be oxidized by molecular oxygen to afford a DNA cleaving copper-oxo species via the intermediacy of $\text{O}_2^{\cdot-}$ and H_2O_2 (Scheme 1), explaining the inhibitory roles of catalase and bathocuproine in the process.

2.3. Lipid peroxidation capacity of **1**

The nuclease property of **1** would be better utilized if its membrane permeability were good. Earlier, the lipid peroxidation capacity of copper–phenolic conjugates has been studied to explain their role in Parkinson's disease as well as bactericidal and anti-cancer properties.^{17a,17b,17c} However, a similar pro-lipid peroxidative activity of tripyrroles is not reported so far. Hence, the lipid peroxidation capacity of **1** was assessed by measuring the TBARS formed in its reaction with the *Escherichia coli* cells in the presence of Cu(II) . The results shown in Figure 5 reveal that compound **1** (50 μM) alone increased the TBARS concentration, which was marginally reduced in the presence of trace amounts (1 μM) of Cu(II) . Cu(II) alone did not lead to significant lipid peroxidation even at a concentration of 50 μM . However, the presence of equimolar concentrations (50 μM) of both, compound **1** and Cu(II) , drastically increased the TBARS production



Figures in parenthesis indicate concn in μM

Figure 5. The extent of TBARS formation via lipid peroxidation in *E. coli* cells by **1** (50 μM), Cu(OAc)_2 individually or in combination. The peroxidation was carried out for 2 h using Cu(OAc)_2 at two different concentrations (1 and 50 μM). Other conditions are as described in Section 4. The values are means \pm SE ($n = 5$).

Table 2. TBARS absorbances due to the lipid peroxidation in *E. coli* by **1** and Cu(OAc)_2 , individually or in combination

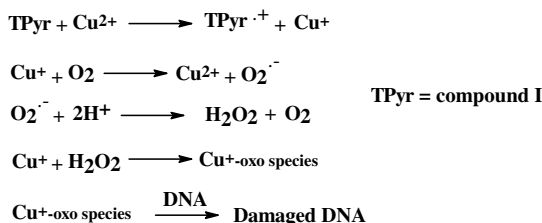
Treatment	TBARS absorbances
Untreated cells	0.019 ± 0.006
Cells + Cu(II) (1 μM)	0.016 ± 0.004
Cells + 1 (50 μM)	0.039 ± 0.024
Cells + Cu(II) (1 μM) + 1 (50 μM)	0.028 ± 0.012
Cells + Cu(II) (50 μM)	0.031 ± 0.004
Cells + Cu(II) (50 μM) + 1 (50 μM)	0.154 ± 0.062

The values are means \pm SE ($n = 5$).

(Table 2). The results confirmed that compound **1**, in conjunction with Cu(II) , can cause membrane damage through lipid peroxidation.

2.4. Cytotoxic property of **1**

It is anticipated that a copper dependent nuclease agent can cause lethal DNA damage due to the significant concentration of copper bound to DNA.¹⁸ In a cellular system, the copper/hydrogen peroxide dependent damage is enhanced by packaging of DNA as a nucleosome.^{14b} A 3.5-fold increase in copper concentration has been reported in cancerous tissue compared to its non-cancerous counterpart.¹⁸ In this context, it was pertinent to evaluate the cytotoxic effect of **1** against tumour cell lines. Hence, its cytotoxic property against EL4 (mouse blood lymphoma) and K562 (human chronic myeloid leukaemia) cell lines was also evaluated. The tripyrrole **1** inhibited the proliferation of both these cell lines in a concentration dependent manner as revealed by the MTT assay. The tripyrrole was more effective against the EL4 cell line compared to the K562 cell line (Fig. 6). For example, at the concentrations of 5, 10 and 25 μM , it showed significant inhibition (59%, 68% and 79%) of the EL4 cell line. In contrast, its inhibitory capacity for the K562 cell line was 11%, 28% and 42%, respectively, at the designated concentrations.



Scheme 1.

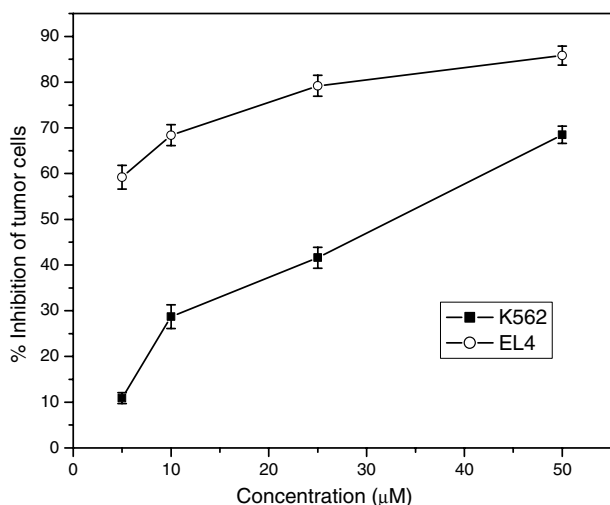


Figure 6. Anti-tumour property of tripyrrole. Human (K562) and mouse (EL4) tumour cell lines were seeded in RPMI 1640 medium at 2×10^5 cells/mL in the presence of different concentrations of **1**. At the end of 48 h incubation at 37 °C in a 5% CO₂ atmosphere the number of viable cells was determined by the MTT assay. Values are means \pm SE ($n = 4$).

3. Conclusion

The importance of the 'A' and 'B' pyrrole rings in the nuclease activity of the prodigiosins has been established recently.¹⁹ The study revealed that replacing the pyrrole moiety in these rings with other heterocycles or aromatic moieties reduced the nuclease activity significantly. Compared to the prodigiosins, the 'A' and 'B' rings of the tripyrrole **1** were not conjugated. From that perspective, the present finding that the Cu(II)–**1** combination can effectively induce dsDNA damage is intriguing and novel. Further, its capability to permeate cellular membranes easily and rupture it by oxidation would be important for its possible nuclease action in cells. Given that dsDNA damage is difficult to repair, compound **1** appears to be a promising candidate as a cytotoxic and anti-tumour agent.^{20a,b} This was also substantiated by the impressive anti-tumour activity of **1**. Finally, although a large number of well characterized A–T-specific DNA binding agents are reported,²¹ compounds that recognize the G–C sequence are rare. As mentioned earlier, the prodigiosins are presently valued as potential anti-cancer agents and various synthetic analogues of them have been evaluated to understand their mechanism of action.⁴ To this end, the present finding that new natural sources can provide novel prodigiosin analogues like **1** with impressive bioactivity is very encouraging. However, the finding that the DNA binding capacities of tripyrroles can be tuned by subtle structural changes is possibly most revealing. This might be useful for designing and synthesizing new drugs with higher potency.

4. Experimental

4.1. Chemicals

Compound **1** was isolated from the *Micrococcus* sp. and fully characterized from its spectral data as reported.⁵

Human K562 and EL4 cell lines were procured from National Centre for Cell Sciences, Pune, India. Hepes buffer, superoxide dismutase (SOD), RPMI 1640 medium, foetal bovine serum (all from Sigma, USA), Cu(OAc)₂ (Aldrich, USA), ethidium bromide (SRL, India) and bathocuproine (HiMedia, India) were used as received. The pBR322 DNA, poly[A–T]₂ decamer and poly[G–C]₂ decamer were obtained from Bangalore Genei Ltd, India. Calf thymus DNA (CT DNA, Sigma, USA) was sonicated and phenol-extracted prior to use. The DNA concentrations were determined using appropriate molar extinction coefficients: $\epsilon_{260} = 12,824 \text{ M}^{-1} \text{ cm}^{-1}$ in base pair (bp) for CT DNA, $\epsilon_{254} = 8400 \text{ M}^{-1} \text{ cm}^{-1}$ in bp for poly[G–C]₂, and $\epsilon_{254} = 6800 \text{ M}^{-1} \text{ cm}^{-1}$ in bp for poly[A–T]₂.⁷

4.2. Spectrophotometry

The absorbance spectroscopy was carried out at 25 °C using a Jasco V-550 UV–vis spectrophotometer. Wavelength scans and absorbance measurements were made in 1 mL quartz cells of 1-cm path length.

4.3. DNA binding assay

4.3.1. Absorption spectrophotometry. This was carried out spectrophotometrically as reported earlier.⁵ A buffered solution of **1** (20 μM) in 100 mM NaCl and 10 mM Hepes buffer, pH 7.2 (total volume 500 μL) was titrated with the DNA solutions. The titrations were carried out using 0.28 μM bp aliquots of CT DNA, 0.38 μM bp aliquots of poly[A–T]₂ and 0.14 μM bp aliquots of poly[G–C]₂. An appropriate vehicle was used in the reference cuvette.

4.3.2. Fluorescence quenching of ethidium bromide (EB). A small aliquot of EB (0.1 mM) was added to CT DNA (0.1 mM) in 10 mM Hepes buffer with 100 mM NaCl and the fluorescence was measured at emission 600 nm after excitation at 530 nm. The experiment was repeated with 0.1 mM CT DNA previously treated with 0.1 mM tripyrrole to ensure its binding with the DNA. The reduction in the fluorescent intensity is expressed as the percentage of that of control (CT DNA + EB).

4.3.3. Viscometry studies. The viscosity of CT DNA solutions was measured at 30 ± 1 °C using an Ubbelohde viscometer. Typically, 3.0 mL of 10 mM Hepes buffer with 100 mM NaCl was transferred to the viscometer to obtain reading of the flow time. For determination of the solution viscosity, 3.0 mL of buffered solution of 0.2 mM CT DNA was taken to the viscometer and a flow time reading was obtained. Different amounts of tripyrrole were added to the CT DNA solution in the same buffer to give appropriate R ([compound **1**]/[DNA base pairs]) values. The flow times of the samples were measured after achieving a thermal equilibrium (30 min). Each point measured was the average of at least three readings with a SD of less than $\pm 1\%$. The data obtained are presented as (η/η_0) versus R , where η is the reduced specific viscosity of CT DNA in the presence of **1** and η_0 is the reduced specific viscosity of CT DNA alone.^{22a,22b}

4.4. DNA nicking assay⁹

The reaction mixtures (total volume 20 μ L) containing Cu(OAc)₂ (50 μ M) and pBR322 plasmid DNA (200 ng) in 10 mM Hepes buffer, pH 7.4, 75 mM NaCl and 10 vol % acetonitrile were incubated at 37 °C for 60 min as such or in the presence of **1** (50 μ M). After adding the DNA gel loading dye (0.25% bromophenol blue, 50% glycerol and 500 μ M EDTA), the samples were loaded in an agarose gel and subjected to electrophoresis at 72 V for 2 h. The DNA gels were visualized under UV light after staining with ethidium bromide (0.5 μ g/mL) for 30 min and quantified by Bio-Rad gel documentation system. For testing the effects of different factors, suitable scavengers were added. For the time dependent experiments, incubation was carried out for 0–120 min.

4.5. Detection of alkali labile sites

This experiment²³ was performed as above using **1** (100 μ M). The reaction was terminated after incubating for 15 and 30 min by the addition of 50 mM EDTA (2 μ L of 0.5 M solution) and 0.5 N NaOH. The mixture was incubated at room temperature for 2 h and the different forms of the DNA were separated as above.

4.6. Copper chelation study

Copper chelation study was carried out by recording the UV–vis spectra (190–600 nm) of a solution of **1** (50 μ M) in 10 mM Hepes, pH 7.2, as such and after adding cupric acetate (50 μ M) solution. The copper chelation was evaluated from the change in absorbance and/or spectral shift.

4.7. Detection of lipid peroxidation products

Escherichia coli grown to late logarithmic phase was harvested by centrifugation, washed with equal volume of 10 mM Hepes, pH 7.2, and 1 mM MgCl₂ and re-suspended in the same. The cells (volume 0.5 mL) were incubated with cupric acetate, **1**, or both for 2 h at 37 °C, 1 mL TBA (0.375%)/TCA (15%)/HCl (0.25 N) solution added and the mixture was incubated at 100 °C for 20 min. After centrifuging at 10,000 rpm for 5 min, the absorbances due to the TBARS in the supernatant were measured at 532 nm.

4.8. Cell culture

Human K562 (chronic myeloid leukaemia) and EL4 (mouse blood lymphoma) were maintained in RPMI 1640 medium supplemented with 10% heat-inactivated foetal bovine serum and 2 mM glutamine, and kept in a humidified incubator at 37 °C with 95% air and 5% CO₂.

4.9. Assessment of cell viability by MTT assay

The cells were harvested by centrifugation, counted and plated in microtitre plates and incubated at 37 °C in 5% CO₂ for 48 h with vehicle ethanol and different

concentrations of **1**. The number of viable cells was determined using the MTT assay as previously described.²⁴

References and notes

- Dupureur, C.; Barton, J. K. In Lehn, J.-M., Ed.; Comprehensive Supramolecular Chemistry; Pergamon: New York, 1997; Vol. 5, p 295.
- Norden, B.; Lincoln, P.; Akerman, B.; Tuite, E. In Sigel, A., Sigel, H., Eds.; Metal Ions in Biological Systems: Probing of Nucleic Acids by Metal Ion Complexes of Small Molecules; Marcel Dekker: New York, 1996; Vol. 33, p 177.
- Wilson, W. D.; Li, Y.; Veal, J. M. *Adv. DNA Specific Reagents* **1992**, *1*, 89.
- Manderville, R. A. *Curr. Med. Chem. Anti-Cancer Agents* **2001**, *2*, 195–218.
- Variyar, P. S.; Chander, R.; Venkatachalam, S. R.; Bongirwar, D. R. *Indian J. Chem. B* **2002**, *41*, 232–233.
- Patil, A. O.; Heeger, A. J.; Wudl, F. *Chem. Rev.* **1988**, *88*, 183–200.
- Melvin, M. S.; Ferguson, D. C.; Lindquist, N.; Manderville, R. A. *J. Org. Chem.* **1999**, *64*, 6861–6869.
- Borah, S.; Melvin, M. S.; Lindquist, N.; Manderville, R. A. *J. Am. Chem. Soc.* **1998**, *120*, 4557–4562.
- Subramanian, M.; Sadakshari, U.; Chattopadhyay, S. *Bioorg. Med. Chem.* **2004**, *12*, 1231–1237.
- (a) Gaecintov, N. E.; Cosman, M.; Mao, B.; Alfano, A.; Hingerty, B. E.; Ibanez, V.; Harvey, R. G. *Carcinogenesis* **1991**, *12*, 2099–2108; (b) Pradhan, P.; Jernstrom, B.; Seidel, A.; Norden, B.; Graslund, A. *Biochemistry* **1998**, *37*, 4664–4673.
- Haq, I.; Lincoln, P.; Suh, D.; Norden, B.; Chowdhry, B. Z.; Chaires, J. B. *J. Am. Chem. Soc.* **1995**, *117*, 4788–4796.
- (a) Baguley, B. C.; LeBret, M. *Biochemistry* **1984**, *23*, 937–943; (b) Lakowicz, J. R.; Webber, G. *Biochemistry* **1973**, *12*, 4161–4170.
- (a) Norden, B.; Tjerneld, T. *Biopolymers* **1982**, *21*, 1713–1734; (b) Lerman, L. *J. Mol. Biol.* **1961**, *3*, 18–30; (c) Kelly, T. M.; Tossi, A. B.; McConnell, D. J.; Streckas, T. C. *Nucleic Acids Res.* **1985**, *13*, 6017–6034.
- (a) Perez-Tomas, R.; Montaner, B.; Llagostera, E.; Soto-Cerrato, V. *Biochem. Pharmacol.* **2003**, *66*, 1447–1452; (b) Melvin, M. S.; Wootton, K. E.; Rich, C. C.; Saluta, G. R.; Kucera, G. L.; Lindquist, N.; Manderville, R. A. *J. Inorg. Biochem.* **2001**, *87*, 129–135.
- (a) Wilson, W. D.; Tanious, F. A.; Barton, H. J.; Jones, R. L.; Streckowski, L.; Boykin, D. W. *J. Am. Chem. Soc.* **1989**, *111*, 5008–5010; (b) Wilson, W. D.; Tanious, F. A.; Ding, D.; Kumar, A.; Boykin, D. W.; Colson, P.; Houssier, C.; Bailly, C. *J. Am. Chem. Soc.* **1998**, *120*, 10310–10321.
- (a) Povirk, L. F.; Wuber, W.; Kohnlein, W.; Hutchinson, F. *Nucleic Acid Res.* **1977**, *4*, 3573–3580; (b) Drak, J.; Iwasawa, N.; Danishefsky, S.; Crothers, D. M. *Proc. Natl. Acad. Sci. USA* **1991**, *88*, 7464–7468.
- (a) Sotomatsu, A.; Nakano, M.; Hirai, S. *Arch. Biochem. Biophys.* **1990**, *283*, 334–341; (b) Ikigai, H.; Nakae, T.; Hara, Y.; Shimamura, T. *Biochem. Biophys. Acta* **1993**, *1147*, 132–136; (c) Hayakawa, F.; Kimura, T.; Maeda, T.; Fujita, M.; Sohmiya, H.; Fuji, M.; Ando, T. *Biochim. Biophys. Acta* **1997**, *1336*, 123–131.
- Liang, Q.; Dedon, P. C. *Chem. Res. Toxicol.* **2001**, *14*, 416–422.
- Furstner, A.; Grabowski, E. J. *ChemBioChem* **2001**, *9*, 706–709.

20. (a) Melvin, M. S.; Tomlinson, J. T.; Saluta, G. R.; Kucera, G. L.; Lindquist, N.; Manderville, R. A. *J. Am. Chem. Soc.* **2000**, *122*, 6333–6334; (b) Jacobi, H.; Eicke, B.; Witte, J. *Free Radic. Biol. Med.* **1998**, *24*, 972–978.
21. Bailly, C. In Palumbo, M., Ed.; *Advances in DNA Specific Agents*; Jai Press: Greenwich, CT, 1998; Vol. 3, pp 97–156.
22. (a) Banville, D. L.; Marzilli, L. G.; Strickland, J. A.; Wilson, W. D. *Biopolymers* **1986**, *25*, 1837–1858; (b) Gray, T. A.; Yue, K. T.; Marzilli, L. G. *J. Inorg. Biochem.* **1991**, *41*, 205–219.
23. Chang, C. H.; Meares, C. F. *Biochemistry* **1982**, *21*, 6332–6334.
24. Basu, A.; Teicher, B. A.; Lazo, J. S. *J. Biol. Chem.* **1990**, *265*, 8451–8457.